IEEE Photonics Journal
An IEEE Photonics Society Publication

Improved Single-Mode Property of DFB Semiconductor Laser Based on Sampling Technique Using Chirp Compensation

Volume 7, Number 1, February 2015

Yuechun Shi
Jilin Zheng
Naizhuo Jiang
Lianyan Li
Yunshan Zhang
Bocang Qiu
Xiangfei Chen, Senior Member, IEEE

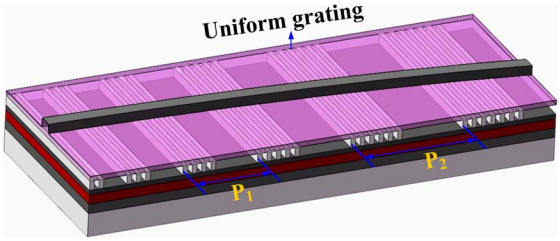

DOI: 10.1109/JPHOT.2014.2381655
1943-0655 © 2014 IEEE

Improved Single-Mode Property of DFB Semiconductor Laser Based on Sampling Technique Using Chirp Compensation

Yuechun Shi,[1] Jilin Zheng,[1,2] Naizhuo Jiang,[1] Lianyan Li,[1,3] Yunshan Zhang,[1,4] Bocang Qiu,[5] and Xiangfei Chen,[1] *Senior Member, IEEE*

[1]Microwave-Photonics Technology Laboratory, National Laboratory of Microstructures and School of Engineering and Applied Sciences, Nanjing University, Nanjing 210093, China
[2]Photonics Information Technology Laboratory, Institute of Communication Engineering, PLA University of Science and Technology, Nanjing 210007, China
[3]Photonics Research Group, Department of Information Technology (INTEC), Ghent University, 9000 Ghent, Belgium
[4]High-Tech Institute of Nanjing University (Suzhou), Suzhou 215123, China
[5]Suzhou Institute of Nano-Tech and Nano-Bionics, Chinese Academy of Sciences, Suzhou 215123, China

DOI: 10.1109/JPHOT.2014.2381655

Manuscript received November 26, 2014; accepted December 3, 2014. Date of publication December 18, 2014; date of current version January 14, 2015. This work was supported by the National Nature Science Foundation of China under Grant 61090392 and Grant 61435014; the Technology Support Program of Jiangsu Province BE2012157; the National "863" project under Grant 2011AA010300; the Natural Science Foundation for the Youth under Grant 61306068; and Natural Science Foundation of Jiangsu Province of Youth under Grant BK20130585 and Grant BK20140414.
Corresponding author: J. Zheng (e-mail: zhengjl@nju.edu.cn).

Abstract: A DFB semiconductor laser with a bent waveguide and an equivalent chirp compensation based on the sampled grating technique is proposed to improve the single longitudinal mode (SLM) performance for the first time. In such a structure, the bent waveguide is used to form the basically chirped grating so that the zeroth-order resonance is greatly suppressed. However, for the −first-order resonance, the equivalent chirp by designing the sampling pattern is used to compensate the chirp in the −first subgrating caused by bent waveguide. As a result, the −first-order resonance is enhanced, whereas the zeroth resonance is well suppressed. Since the wavelength spacing between the zeroth and −first subgrating can be reduced by adopting this method, the sampling period can be increased. Therefore, the corresponding line in photomask can be enlarged as well to ease the fabrication, and the lasing wavelength accuracy can be further improved according to the theoretical analysis. Because the lasing wavelength can be controlled by changing the sampling period, the performances of the multiwavelength DFB laser array can also be improved using this method.

Index Terms: DFB semiconductor laser, sampled grating, bent waveguide.

1. Introduction

Multi-wavelength DFB laser arrays (MLAs) are the key elements in photonic integrated circuits (PICs) and high-speed optical communication systems [1]–[4]. For an MLA that meets Wavelength Division Multiplexing (WDM) requirements, single longitudinal mode (SLM) must be guaranteed for all lasers and the lasing wavelengths have to be accurately controlled. As a result, the structures as fine as to nano-scale, such as those for phase shift or chirp, are required in

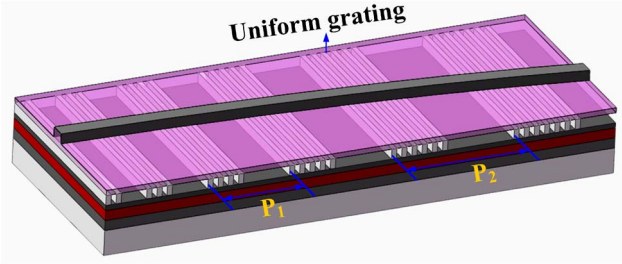

Fig. 1. Schematic of the proposed structure with a bent waveguide and pre-designed sampling patterns for equivalent chirp. P_1 and P_2 are the sampling periods.

the Bragg gratings of DFB lasers to ensure SLM operation. The grating periods of each laser need to be precisely produced. For example, wavelength spacing of 0.8 nm requires a grating period difference of around 0.125 nm. Up to now, the fabrication is usually carried out using E-beam lithography (EBL) which can write arbitrary grating patterns. However, it suffers from time consumption, high cost, and unavoidable stitching errors [5]. The reconstruction-equivalent-chirp (REC) technique, which is based on the sampled grating, has recently been proposed and has been successfully applied to fabricate different DFB lasers and laser arrays [6]–[8]. In REC technique, the sampling patterns are carefully designed to realize the desired grating profile in some subgratings (usually the +first/−first subgrating) equivalently. It has some advantages such as high wavelength precision and low fabrication cost [7], [9], [10]. However, since sampled gratings have multi-channel (subgrating) reflections [11], the zeroth order resonance can lead to undesirable lasing. Consequently, the sampling period is usually designed small enough in order to shift the zeroth order wavelength far away from the gain region. However, lasing of the zeroth order wavelength may still occur when the gain spectrum is shifted due to material growth variations or other reasons such as the temperature. Therefore, a number of methods are proposed to suppress the zeroth subgrating resonance or to increase the wavelength spacing between the zeroth and +first/−first subgrating [12]–[14]. However, the fabrication process is much more complex.

In this paper, a new method to suppress the zeroth order resonance and enhance the −first order resonance is proposed for the first time. The bent waveguide is designed to form the basic chirped grating (seed grating) to reduce the zeroth order resonance. The equivalent chirp is designed simultaneously to compensate the chirp in the −first subgrating which is used as the resonator, and an equivalent π phase shift is inserted in order to realize SLM operation around the −first Bragg wavelength. Besides, the multi-wavelength DFB laser arrays can be realized by designing different sampling periods. The proposed method is compatible to the current laser fabrication process, so the process cost is as low as that for processing normal DFB lasers.

2. Principle

The proposed structure with a bent waveguide and pre-designed sampling patterns is schematically shown in Fig. 1. The bent waveguide is used to form the basic (seed) chirped grating and the non-uniform sampling pattern is designed to form a reversed equivalent chirp profile to compensate the chirp in a particularly desired order sub-grating (usually the ±first order).

2.1. Grating Period Variation

The grating period $\Lambda_{\text{bent}}(z)$ along a bent waveguidecan be expressed as a function of the tilt angle $\theta(z)$ as follows [15], [16]:

$$\Lambda_{\text{bent}}(z) = \frac{\Lambda_0}{\cos\theta(z)} \tag{1}$$

where Λ_0 is the uniform grating period. As a result, the chirped grating period profile can be achieved by carefully designing the tilt angle along the waveguide.

2.2. Chirp Compensation

Once we obtain the chirped grating, the seed grating with chirped profile for REC technique is also achieved. If the chirp coefficient is C, then the grating period distribution can be expressed as

$$\Lambda(z) = \Lambda_0 + Cz. \tag{2}$$

Hence, the grating refractive index modulation can be expressed as

$$\Delta n(z) = \frac{1}{2}\Delta n \exp\left(\int j\frac{2\pi}{\Lambda(z)}dz\right) + c.c \approx \frac{1}{2}\Delta n \exp\left(-j\frac{\pi Cz^2}{\Lambda_0^2}\right)\exp\left(j\frac{2\pi z}{\Lambda_0}\right) + c.c \tag{3}$$

where Δn is the refractive index modulation depth.

The uniform sampling pattern can be expanded into a *Fouier-Series*

$$S(z') = \sum_m F_m \exp\left(j\frac{2\pi m}{P}z'\right) \tag{4}$$

where P is the sampling period. Furthermore, in order to analyze a sampling pattern with arbitrary period, (4) can be written as

$$S(z) = \sum_m F_m \exp\left[j\frac{2\pi m}{P}f(z)\right] \tag{5}$$

where $z' = f(z)$. Here, the transformation of coordinates is applied and $f(z)$ is an arbitrary function that relates to the sampling pattern. In order to simplify the analysis, it is further changed into

$$f(z) = z + \varphi(z) \tag{6}$$

Apparantly, if $\varphi(z) = 0$, (5) describes a uniform sampling pattern. As a result, the sampled grating with arbitrary sampling pattern can be expressed as

$$\Delta n_s(z) = \frac{1}{2}\Delta n \sum_m F_m \exp\left[j\left(\frac{2\pi m}{P} + \frac{2\pi}{\Lambda_0}\right)z\right]\exp\left[j\frac{2\pi m\varphi(z)}{P}\right]\exp\left(-j\frac{\pi Cz^2}{\Lambda_0^2}\right) + c.c. \tag{7}$$

For $m = -1$st order subgrating, (7) can be simplified as

$$\Delta n_{s-1}(z) = \frac{1}{2}\Delta n F_{-1} \exp\left[j2\pi\left(\frac{1}{\Lambda_0} - \frac{1}{P}\right)z\right]\exp\left[-j\frac{2\pi\varphi(z)}{P}\right]\exp\left(-j\frac{\pi Cz^2}{\Lambda_0^2}\right) + c.c. \tag{8}$$

If the $-$first order subgrating is used as the operation resonator and the chirp is compensated by sampling pattern, following condition must be met:

$$\frac{2\pi\varphi(z)}{P} + \frac{\pi Cz^2}{\Lambda_0^2} = 0. \tag{9}$$

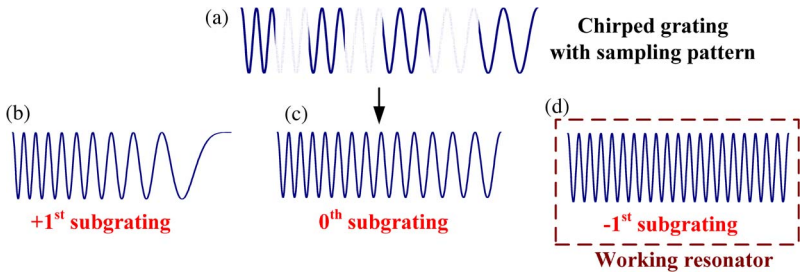

Fig. 2. Schematic illustration of the +first, zeroth, and −first order subgratings in the proposed sampled grating.

From (9), one can see the function $\varphi(z)$ which is related to the sampling pattern $f(z)$, can be written as

$$\varphi(z) = -\frac{Cz^2 P}{2\Lambda_0^2}. \tag{10}$$

Thus, the index modulation of the −first subgrating can be expressed as

$$\Delta n_{s-1}(z) = \frac{1}{2}\Delta n F_{-1} \exp\left[j2\pi\left(\frac{1}{\Lambda_0} - \frac{1}{P}\right)z\right] + c.c. \tag{11}$$

Therefore, an equivalent uniform grating is achieved in the −first order channel. An equivalent π phase shift can also be produced according to the REC technique in order to realize SLM operation around the −first Bragg wavelength.

For $m = 1$st order subgrating, (7) can be simplified as

$$\Delta n_{s+1}(z) = \frac{1}{2}\Delta n F_{+1} \exp\left[j2\pi\left(\frac{1}{\Lambda_0} + \frac{1}{P}\right)z\right] \exp\left[j\frac{2\pi\varphi(z)}{P}\right] \exp\left(-j\frac{\pi Cz^2}{\Lambda_0^2}\right) + c.c. \tag{12}$$

The phase term in (12) is

$$\exp\left[j\frac{2\pi\varphi(z)}{P}\right] \exp\left(-j\frac{\pi Cz^2}{\Lambda_0^2}\right) = \exp\left(-j\frac{\pi C' z^2}{\Lambda_0^2}\right). \tag{13}$$

Here $C' = 2C$, which means the chirp in the +first subgrating is doubled.

For $m = 0$th order subgrating, (7) can be simplified as

$$\Delta n_{s0}(z) = \frac{1}{2}\Delta n F_0 \exp\left[j\frac{2\pi}{\Lambda_0}z\right] \exp\left(-j\frac{\pi Cz^2}{\Lambda_0^2}\right) + c.c. \tag{14}$$

It implies that the zeroth order subgrating profile is the same as the seed grating where the chirp can reduce the reflection and therefore suppress the zeroth order resonance. The results are illustrated in Fig. 2.

2.3. Coupling Coefficient in Bent Waveguide Region

The coupling coefficient is dependent on the tilt angle of the bend waveguide. The formula for the coupling coefficient of a normal 3-D Bragg grating is given in [17]. The normalized coupling coefficient of tilted Bragg grating is derived in the Appendix and expressed as

$$\frac{\kappa(\theta)}{\kappa(0)} = \frac{\int_{-\infty}^{+\infty} \cos\left(\frac{2\pi}{\Lambda_0}\sin\theta x\right) U^2(x, y_0)\,dx}{\int_{-\infty}^{+\infty} U^2(x, y_0)\,dx}. \tag{15}$$

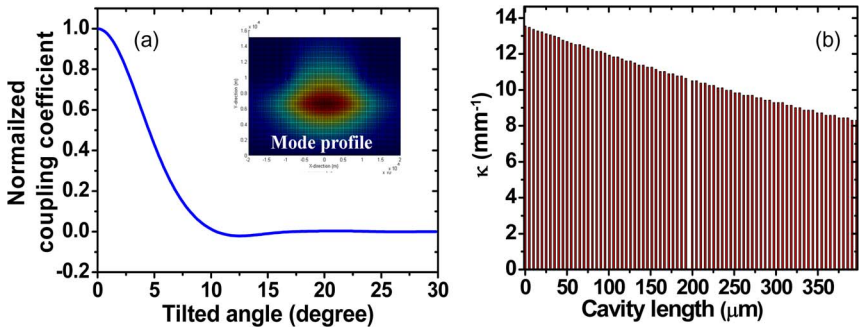

Fig. 3. (a) Calculated curve of (15). The inserted figure is the mode of a common laser with ridge waveguide used in the calculation. (b) The coupling coefficient distribution along cavity calculated by (15) with grating chirp of $1.3e^{-6}$.

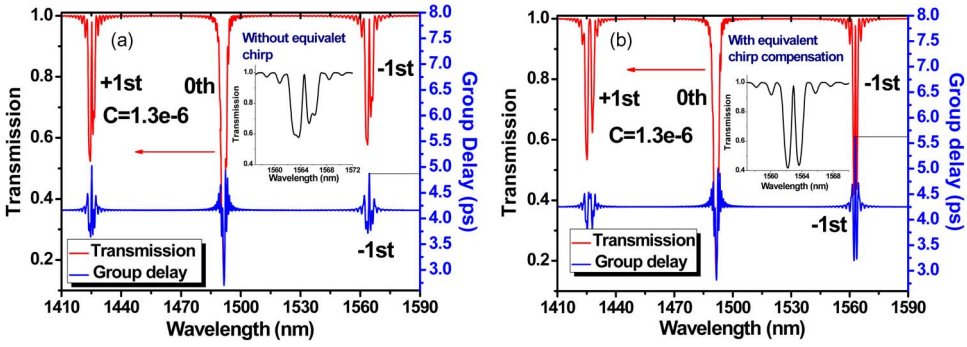

Fig. 4. Calculated transmission spectra and group delays of chirped gratings (a) without equivalent chirp compensation and (b) with equivalent chirp compensation.

The calculated results are shown in Fig. 3. Fig. 3(a) shows the curve of (15) versus the tilt angle. The inserted figure is the mode profile of a normal ridge waveguide which is used in the calculation. Fig. 3(b) is the corresponding coupling coefficient of the sampled grating along cavity with the length of 400 μm calculated using (15). The chirp coefficient is $1.3e^{-6}$. The effect of the varied coupling coefficient along cavity is also considered in the following simulations.

3. Simulation Results

3.1. Passive Grating Cavity Property

In order to verify the effect of the zeroth order suppression by chirp compensation scheme, we designed a waveguide Bragg grating with the proposed structure. The cavity was 400 μm long, the uniform grating period Λ_0 was 232.8 nm, the effective refractive index was 3.2, and the chirp coefficient C was $1.3e^{-6}$. The tilt angle distribution can be calculated using (1). The coupling coefficient distribution is shown in Fig. 3(b). In order to compensate the chirp in the $-$first order subgrating, the sampling periods were designed from 5.0 μm to 5.23 μm according to (7). Therefore, the zeroth order wavelength is around 1490 nm and the $-$first order wavelength is around 1562 nm. Equivalent π phase shift was also inserted in the middle of cavity. In order to make comparisons, a grating without chirp compensation was designed at the same time. The simulations were implemented using transfer matrix method (TMM) [18].

Fig. 4(a) is the calculated transmission spectra and group delay with seed grating chirp but without equivalent chirp compensation. The zeroth order resonance is suppressed to some extent as the result of the chirp profile, but both the reflections of the $+/-$first subgratings are also

TABLE 1

The parameters used in our laser model

Slope of gain-carrier density relationship (a)	2.0×10-16 cm^2
Transparency carrier density (N_t)	1.2×1018 cm^{-3}
Confinement factor (Γ)	0.3
Linewidth enhancement factor (β)	1.5
Linear carrier lifetime (τ)	4 ns
Waveguide loss (α_L)	30 cm^{-1}
Active layer thickness (d)	180 nm
Effective refractive index (N_{eff})	3.20
Waveguide width(W)	2.0 μm

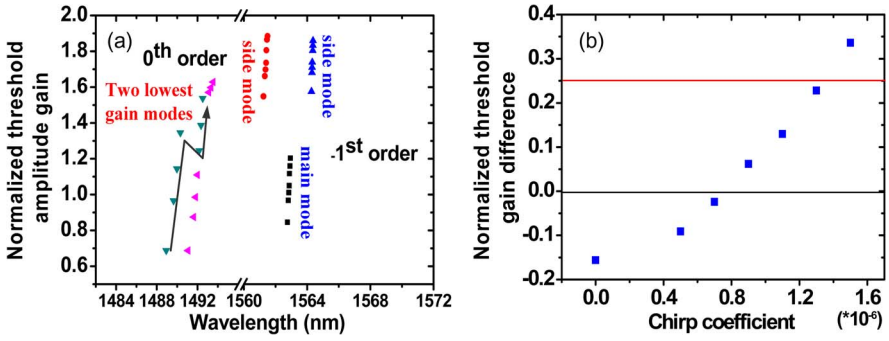

Fig. 5. (a) Calculated normalized threshold amplitude gains for the zeroth order and the −first subgratings. The chirp coefficients are 0, $0.5e^{-6}$, $0.7e^{-6}$, $0.9e^{-6}$, $1.1e^{-6}$, $1.3e^{-6}$, and $1.5e^{-6}$, respectively. All the threshold gains for different modes increase when chirp coefficient increase, except for the short wavelength mode in the zeroth order, which is denoted by a broken line. (b) Normalized threshold gain difference between the lowest gain in the −first and zeroth order subgratings.

reduced and distorted simultaneously. However, when the chirp was compensated in the −first subgrating as is shown in Fig. 4(b), there is no distortions in the −first reflection and the resonance is also enhanced in accordance with the group delay of about 5.6 ps which is compared to only 4.8 ps for that without compensation. The zeroth subgratings in both cases are suppressed due to the chirp induced by the bent waveguide, and the resonance of the +first subgrating with equivalent chirp compensation is suppressed stronger due to the doubled chirp. As is shown in Fig. 4(b), the group delay is much lower than that in Fig. 4(a), which is consistent with the theoretical analysis made above.

3.2. Threshold Condition Analysis

The threshold conditions for proposed DFB lasers were calculated by TMM which is based on the coupling mode model [19]. The parameters of DFB grating are the same as that of the grating with chirp compensation which has been discussed above. The other parameters are listed in Table 1.

Fig. 5(a) shows calculated dependence of normalized threshold gain on the chirp parameters for the zeroth and −first resonance. In the calculation, the chirp coefficient was varied from 0 to $1.5e^{-6}$. As can be seen from Fig. 5(a), threshold gains for the both resonances increase with the increase in the chirp coefficient, and the normalized threshold gain of the zeroth order resonance is much lower than that of the −first order resonance when there is no chirp in the seed gratings, implying that the zeroth order lasing has lower threshold current than that of the −1th order lasing. When the chirp coefficient is larger than $0.8e^{-6}$, the −first threshold gain begins to be lower than that of the zeroth threshold gain. In order to obtain stable SLM operation, the normalized gain difference needs to be larger than 0.25 [17]. Because of this, the chirp coefficient has to be larger than $1.4e^{-6}$ as is shown in Fig. 5(b). However, owing to the fact that the gain

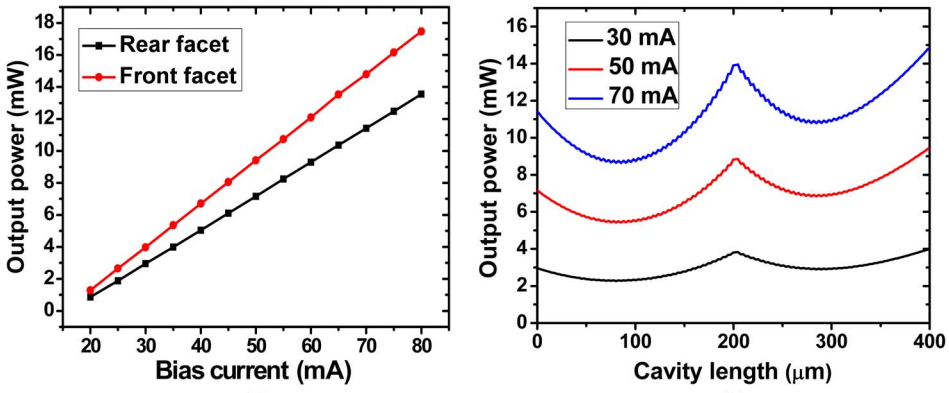

Fig. 6. (a) Calculated P-I curves of front and rear facets and (b) the internal light distributions at currents of 30 mA, 50 mA, and 70 mA, respectively.

spectrum of multiple-quantum-well (MQW) is limited within a certain wavelength region and can be approximately expressed as quadratic form [20], the actual gain for the zeroth order is much lower than the gain of the −first order, because the −first order resonance wavelength was tuned to the peak position of the gain spectrum. Therefore, suppression of the zeroth order lasing could be achieved for chirp coefficients smaller than $1.4e^{-6}$. Whilst the threshold gain of the −first order subgrating resonance becomes smaller for larger chirp coefficients, which is attributed to the decreased and asymmetric coupling coefficient with increased variation in the tilt grating angle for larger chirp coefficient If the zeroth order is suppressed well enough with large chirps, the wavelength spacing between the zeroth and −first wavelength can be significantly reduced according to (11) and (14). As a result, the sampling period can also be much larger than that for normal lasers based on REC technique, which will relax the fabrication process. Moreover, the wavelength precision can be further improved as well, according to the equation described in [7] and [9], and can be expressed as

$$\Delta\Lambda_{-1} = -\frac{1}{\left(\frac{P}{\Lambda_0} - 1\right)^2}\Delta P \tag{16}$$

where ΔP and $\Delta\Lambda_{-1}$ denote the sampling period error and the −first subgrating period error, respectively.

In order to obtain excellent SLM performances, device parameters such as material gain spectrum, the bent angle of the waveguide and the zeroth order wavelength must be fully optimized.

3.3. Laser Performances Above Threshold

The laser performances above threshold were also simulated using TMM method [21]. All the parameters remained identical to that for threshold condition analysis. The power-current (P-I) curves are plotted in Fig. 6(a). Different efficiency slopes of 0.212 W/A and 0.270 W/A were obtained for the front and rear facets of the laser. The difference in the slope efficiency for front and rear facets is attributed to the asymmetric coupling coefficient as is shown in Fig. 3(b). Because the SLM property is not degenerated as was analyzed before, this is advantageous for the integrated laser array sources as more light can be extracted out from one facet [22]. The internal light distributions with different injection current levels are plotted in Fig. 6(b), and clearly more light is accumulated at the front facet, which is in accordance with the P-I curves shown in fig. 6(a).

The laser spectrum is simulated as is shown in Fig. 7(a). The bias current is 30 mA. The gain of the zeroth order around 1490 nm is assumed to be 20% of the gain peak which is around 1550 nm to consider the unflatten gain spectrum. The lasing wavelength in the −first order channel is at the middle of the stopband, which is resulted from the equivalent π phase shift. The zeroth order lasing is significantly suppressed. For the above threshold operation, the dominant

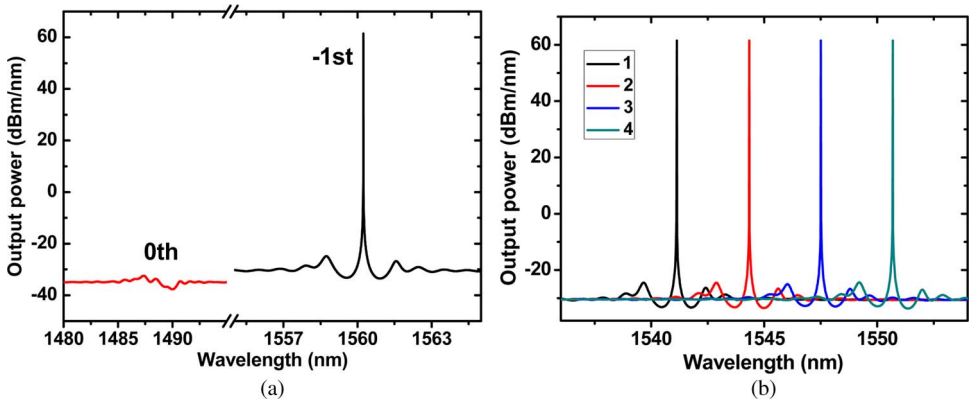

Fig. 7. (a) Calculated lasing spectrum where the magnitude of the gain around 1490 nm is assumed to be 20% of that at 1550 nm. (b) Simulated lasing spectra of a four-wavelength DFB laser array with wavelength spacing of 3.2 nm.

−first lasing can make the zeroth order resonance deviate from the phase match condition apart from the reason of chirped grating. As a result, the suppression of the zeroth order lasing can be further enhanced.

Thanks to the sampling pattern, the multi-wavelength DFB laser arrays can be simply realized by designing different sampling periods. A four-wavelength laser array was simulated with uniform wavelength spacing of 3.2 nm, and the spectra are shown in Fig. 7(b).

4. Discussion

During grating fabrication, the grating period error is usually introduced, which may influence the compensation effect. Therefore, a variation in seed grating phase occurs and can be expressed as $\Delta\phi(z) = \mathrm{j}(2\pi Cz^2/\Lambda_0^2)\Delta\Lambda_0$, while the compensation induced by the sampling pattern is fixed with a phase of $\phi_c(z) = \mathrm{j}(\pi Cz^2/\Lambda_0^2)$, and the ratio between them $\Delta\phi(z)/\phi_c(z)$ is $2\Delta\Lambda_0/\Lambda_0$. Assuming the grating period Λ_0 is 250 nm and fabrication error is 2.0 nm, the ratio is only 0.016. That is to say, the seed grating fabrication errors can be practically ignored, which is very beneficial for the actual applications. In addition, it should be mentioned that bent waveguide can cause radiation loss, but fortunately, it is not severe [15], [16].

5. Conclusion

A novel structure based on REC technique is proposed to improve the SLM operation in DFB lasers. Bent waveguide was used to form chirped grating along the cavity in order to effectively suppress the zeroth order resonance, and equivalent chirp compensation in the −first order subgrating was introduced by sampling technique to enhance resonance of the −first order. The detailed theoretical analysis indicates that very good performances can be achieved. The proposed approach can also benefit the applications of multi-wavelength DFB laser arrays to the future PICs.

Appendix

The top view of the tilted grating with tilt angle of θ is shown in Fig. 8. The relative permittivity corrugation can be expanded in Fourier series as

$$\Delta\varepsilon(x,y,z) = \sum_{q=-\infty}^{\infty} A_{q\neq 0}(x,y,z)\exp(\mathrm{j}\bar{k}\bar{r}) \tag{A.1}$$

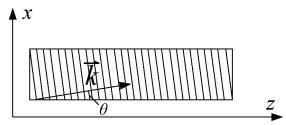

Fig. 8. Top view of a tilted grating with tilted angle of θ.

where, A is the Fourier coefficient, and k is the grating-vector which can be further written as

$$\bar{k} = \frac{2\pi}{\Lambda_0}\cos\theta\bar{e}_z + \frac{2\pi}{\Lambda_0}\sin\theta\bar{e}_x. \tag{A.2}$$

Then, A.1 can be expressed as

$$\Delta\varepsilon(x,y,z) = \sum_{q=-\infty}^{\infty} A_{q\neq 0}(x,y,z)\exp\left(j\frac{2\pi}{\Lambda_0}\cos\theta z\right)\exp\left(j\frac{2\pi}{\Lambda_0}\sin\theta x\right). \tag{A.3}$$

The coupling coefficient for some order Fourier component with tilt angle θ can be expressed as

$$\kappa(\theta) = \frac{k_0^2}{2\beta}\frac{\iint A_{q\neq 0}(x,y,z)\exp\left(\mathrm{j}\frac{2\pi}{\Lambda_0}\sin\theta_x\right)U^2(x,y)\,dx\,dy}{\iint U^2(x,y)\,dx\,dy} \tag{A.4}$$

where $U(x,y)$ is the mode field distribution along the transverse $X-Y$ plane, k_0 is the light wave-vector in vacuum, and β is the mode propagation constant. In the y direction, the Integral height is the grating tooth depth which is assumed to be from d_1 to d_2 with mean depth of d_0. Therefore, (A.4) can be expressed as

$$\kappa(\theta) = \frac{k_0^2}{2\beta}\frac{\int_{d1}^{d2}\int_{-\infty}^{+\infty} A_{q\neq 0}\exp\left(\mathrm{j}\frac{2\pi}{\Lambda_0}\sin\theta_x\right)U^2(x,y)\,dx\,dy}{\iint U^2(x,y)\,dx\,dy}. \tag{A.5}$$

Because the grating depth is very small with only dozens of nanometers, the mode field along grating region in y direction can be considered as uniform. Then $U^2(x,y)$ in grating region can be approximated as $U^2(x,y_0)$ which is the field distribution at y_0. As a result, the integral component related to y is a constant C and (A.5) is written as

$$\kappa(\theta) = \frac{k_0^2}{2\beta}\frac{\int_{d1}^{d2}\int_{-\infty}^{+\infty} A_{q\neq 0}\exp\left(j\frac{2\pi}{\Lambda_0}\sin\theta x\right)U^2(x,y_0)\,dx\,dy}{\iint U^2(x,y)\,dx\,dy} = \frac{k_0^2}{2\beta}\frac{C\int_{-\infty}^{+\infty} A_{q\neq 0}\exp\left(j\frac{2\pi}{\Lambda_0}\sin\theta x\right)U^2(x,y_0)\,dx}{\iint U^2(x,y)\,dx\,dy} \tag{A.6}$$

and (A.6) can be further expanded as

$$\kappa(\theta) = \frac{k_0^2}{2\beta}\frac{C\int_{-\infty}^{+\infty} A_{q\neq 0}\cos\left(\frac{2\pi}{\Lambda_0}\sin\theta x\right)U^2(x,y_0)\,dx}{\iint U^2(x,y)\,dx\,dy} + \mathrm{j}\frac{k_0^2}{2\beta}\frac{C\int_{-\infty}^{+\infty} A_{q\neq 0}\sin\left(\frac{2\pi}{\Lambda_0}\sin\theta x\right)U^2(x,y_0)\,dx}{\iint U^2(x,y)\,dx\,dy}. \tag{A.7}$$

Because $\sin((2\pi/\Lambda_0)\sin\theta x)$ is an odd function, the integral of imaginary part approaches zero, and then, (A.7) is expressed as

$$\kappa(\theta) \cong \frac{k_0^2}{2\beta}\frac{C\int_{-\infty}^{+\infty} A_{q\neq 0}\cos\left(\frac{2\pi}{\Lambda_0}\sin\theta x\right)U^2(x,y_0)\,dx}{\iint U^2(x,y)\,dx\,dy} \tag{A.8}$$

Finally, the normalized coupling coefficient related to tilt angle θ can be written as

$$\frac{\kappa(\theta)}{\kappa(0)} \cong \frac{\int_{-\infty}^{+\infty} \cos\left(\frac{2\pi}{\Lambda_0}\sin\theta x\right) U^2(x, y_0)\, dx}{\int_{-\infty}^{+\infty} U^2(x, y_0)\, dx}. \tag{A.9}$$

References

[1] L. Hou, M. Haji, J. Akbar, J. H. Marsh, and A. C. Bryce, "AlGaInAs/InP monolithically integrated DFB laser array," *IEEE J. Quantum Electron.*, vol. 48, no. 2, pp. 137–143, Feb. 2012.

[2] W. Li, X. Zhang, and J. Yao, "Experimental demonstration of a multi-wavelength distributed feedback semiconductor laser array with an equivalent chirped grating profile based on the equivalent chirp technology," *Opt. Exp.*, vol. 21, no. 17, pp. 19 966–19 971, Sep. 2013.

[3] J. Zhao *et al.*, "Experimental demonstration of a 16-channel DFB laser array based on nanoimprint technology," *Semicond. Sci. Technol.*, vol. 28, no. 5, May 2013, Art. ID. 055015.

[4] C. Zhang, S. Liang, H. Zhu, B. Wang, and W. Wang, "A modified SAG technique for the fabrication of DWDM DFB laser arrays with highly uniform wavelength spacings," *Opt. Exp.*, vol. 20, no. 28, pp. 29 620–29 625, Dec. 2012.

[5] T. Kjellberg and R. Schatz, "The effect of stitching errors on the spectral characteristics of DFB lasers fabricated using electron beam lithography," *J. Lightw. Technol.*, vol. 10, no. 9, pp. 1256–1266, Sep. 1992.

[6] J. Li *et al.*, "Experimental demonstration of distributed feedback semiconductor lasers based on reconstruction-equivalent-chirp technology," *Opt. Exp.*, vol. 17, no. 7, pp. 5240–5245, Mar. 2009.

[7] Y. Shi *et al.*, "Experimental demonstration of eight-wavelength distributed feedback semiconductor laser array using equivalent phase shift," *Opt. Lett.*, vol. 37, no. 16, pp. 3315–3317, Aug. 2012.

[8] L. Li *et al.*, "Experimental Demonstration of a Low-cost Tunable Semiconductor DFB Laser for Access Networks," *Semicond. Sci. Technol.*, vol. 29, no. 9, Sep. 2014, Art. ID. 095002.

[9] Y. Shi *et al.*, "Study of the multiwavelength DFB semiconductor laser array based on the reconstruction-equivalent-chirp technique," *J. Lightw. Technol.*, vol. 31, no. 20, pp. 3243–3250, Oct. 2013.

[10] Y. Shi *et al.*, "High channel count and high precision channel spacing multi-wavelength laser array for future PICs," *Sci. Rep.*, vol. 4, Dec. 2014, Art. ID. 7377.

[11] X. Chen, Y. Luo, C. Fan, T. Wu, and S. Xie, "Analytical expression of sampled Bragg gratings with chirp in the sampling period and its application in dispersion management design in a WDM System," *IEEE Photon. Technol. Lett.*, vol. 12, no. 8, pp. 1013–1015, Aug. 2000.

[12] S. Bao, Y. Xi, S. Zhao, and X. Li, "Sampled grating DFB laser array by periodic injection blocking," *IEEE, J. Sel. Top. Quant. Electron.*, vol. 19, no. 5, Sep./Oct. 2013, Art. ID. 1503008.

[13] Y. Shi *et al.*, "An anti-symmetric-sample grating structure for improving the reconstruction-equivalent-chirp technology," *IEEE Photon. Technol. Lett.*, vol. 23, no. 18, pp. 1337–1339, Sep. 2011.

[14] Y. Zhou, Y. Shi, S. Li, S. Liu, and X. Chen, "Asymmetrical sampling structure to improve the single-longitudinal-mode property based on reconstruction-equivalent-chirp technology," *Opt. Lett.*, vol. 35, no. 18, pp. 3123–3125, Sep. 2010.

[15] H. Hillmer, K. Magari, and Y. Suzuki, "Chirped gratings for DFB laser diodes using bent waveguides," *IEEE Photon. Tech. Lett.*, vol. 5, no. 1, pp.10–12, Jan. 1993.

[16] H. Hillmer and B. Klepser, "Low-cost edge-emitting DFB laser arrays for DWDM communication systems implemented by bent and tilted waveguides," *IEEE J. Quantum Electron.*, vol. 40, no. 10, pp. 1377–1383, Oct. 2004.

[17] H. Ghafouri-Shiraz, *Distributed Feedback Laser Diodes and Optical Tunable Filters*. Hoboken, NJ, USA: Wiley, 2003.

[18] M. Yamada and K. Sakuda, "Analysis of almost-periodic distributed feedback slab waveguides via a fundamental matrix approach," *Appl. Opt.*, vol. 26, no. 16, pp. 3474–3478, Aug. 1987.

[19] C. F. Fernandes, "Threshold analysis of phase-shifted distributed feedback lasers," *Proc. 9th Mediterranean Electrotech. Conf. MELECON*, 1998, pp. 1436–1439.

[20] K. Petermann, "Longitudinal mode spectrum of lasing emission," in *Laser Diode Modulation Noise*. Dordrecht, The Netherlands: Kluwer, 1988.

[21] G. P. Agrawal and A. H. Bobeck, "Modeling of distributed feedback semiconductor lasers with axially-varying parameters," *IEEE J. Quantum. Electron.*, vol. 24, no. 12, pp. 2407–2414, Dec. 1988.

[22] O. K. Kwon *et al.*, "Effects of asymmetric grating structures on output efficiency and single longitudinal mode operation in $\lambda/4$-shifted DFB laser," *IEEE, J. Quantum. Electron.*, vol. 47, no. 9, pp. 1185–1194, Sep. 2011.